

RADIATION DISTRIBUTION AND POWER BALANCE IN THE ASDEX UPGRADE LYRA DIVERTOR

J.C. Fuchs, K.F. Mast, D. Coster, A. Herrmann, M. Münch, R. Schneider,
and the ASDEX Upgrade Team

MPI für Plasmaphysik, EURATOM-Association, D-85748 Garching, Germany

1. Introduction

Radiation losses in the new Lyra divertor (DV-II) of ASDEX Upgrade are investigated. A detailed knowledge of the radiation distribution in the divertor is necessary in order to increase and control the divertor radiation with the aim of reducing the power load on the divertor plates under ITER relevant conditions. Therefore a completely new bolometer diagnostic was designed for the observation of the X-point and divertor region:

Two bolometer pinhole cameras with 7 lines of sight each measure radiation from the inner and outer divertor leg and allow for a correction of the neutral gas pressure dependent bolometer sensitivity and of the residual bolometer offset drift. The region around the X-point is observed with an 8 channel pinhole camera, the main plasma with 72 bolometers placed in five cameras. The bolometers are miniaturized, low noise metal resistor bolometers [1] which are excited by a 50kHz sine wave and effectively suppress thermal drift and electromagnetic interferences.

In order to obtain the distribution of the local radiation emissivity in a poloidal cross section of the plasma, the measured line integrals must be unfolded. This is done with the ‘Anisotropic Diffusion Model Tomography’ algorithm (ADMT), which is based on the fact that the variation of the radiation emissivity along magnetic field lines is much smaller than perpendicular to them. This behaviour is described by an anisotropic diffusion model with different values of the diffusion coefficients D_{\parallel} , D_{\perp} along and perpendicular to the magnetic field lines. [2]

Radiation distributions and power balance have been investigated for a wide variety of plasma regimes. Examples for shots with high heating power will be presented.

2. Radiation Pattern in the LYRA Divertor

The measured line integrals of the 22 divertor bolometer together with the other 72 bolometers of ASDEX Upgrade have been unfolded in order to reconstruct the radiation distribution in the divertor region as well as in the main chamber.

Fig. 1 shows a typical example for the radiation pattern in the ASDEX Upgrade LYRA divertor for a deuterium discharge with 20MW neutral beam injection power in H-mode ($I_p=1\text{MA}$, $\bar{n}_e = 7 \cdot 10^{19}\text{m}^{-3}$, $B_T=-2.5\text{T}$). There are two pronounced peaks of the radiation density in both the inner and outer divertor fan with emissivities of up to 30-40MW/m³. However, due to the limited resolution of the

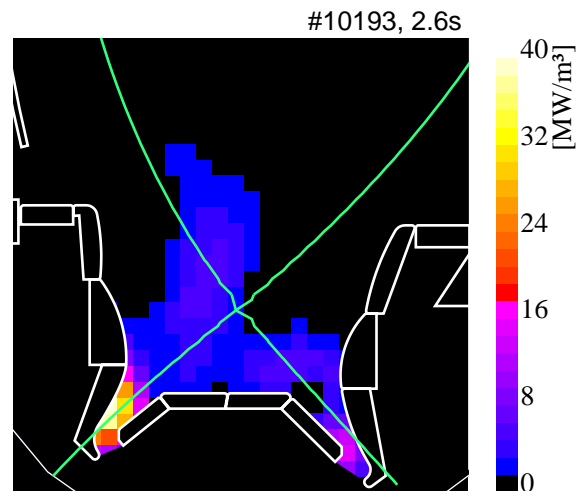


Fig.1: Reconstructed radiation pattern in the ASDEX Upgrade LYRA divertor with pronounced radiation peaks in the inner and outer divertor fan

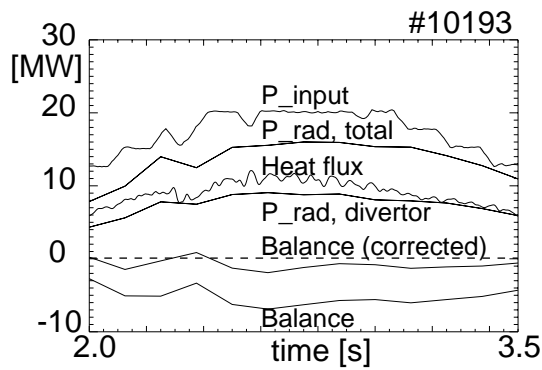


Fig. 2: Power balance for the 20MW discharge from Fig. 1, showing input power, total radiated power, radiated power from divertor, heat flux onto divertor plates measured by thermography, power balance and corrected power balance

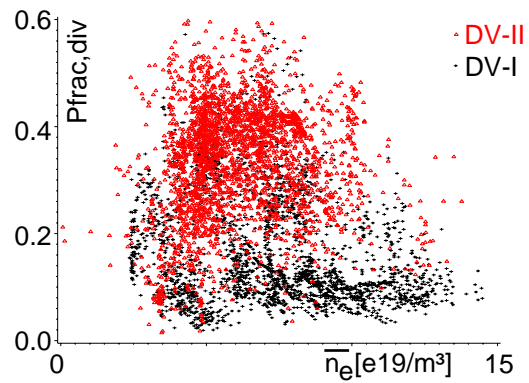


Fig. 3: Fraction of the radiated power in the divertor to the input power as function of line averaged density; black crosses=DV-I, red triangles=DV-II

bolometer lines of sight in horizontal direction in the divertor, the reconstructed radiation density may have been smoothed out by the tomographic algorithm over the width of the fans, and the real emissivity may even be higher and more concentrated. There is also radiation between the strikepoints and the X-point, which will be discussed later more detailed. In the main plasma one finds radiation mainly along the separatrix with emissivities of a few MW/m^3 .

Integrating the radiation emissivity over the whole plasma one finds that the total radiated power is about 60%-80% of the input power (Fig. 2). Radiation from the divertor and X-point region is about 40%-50% of the input power, which is clearly higher than the radiated fraction in DV-I, thus also reducing the power load onto the divertor plates (Fig. 3) [3].

Modeling of the radiation emissivity with the B2-Eirene code predicts a small radiation zone along the separatrix between the strikepoints and the X-point (Fig. 4a), however due to the limited spatial resolution of the bolometer lines of sight these radiation bands cannot be detected in normal plasma discharges. Therefore the plasma was shifted vertically for about 10cm, such

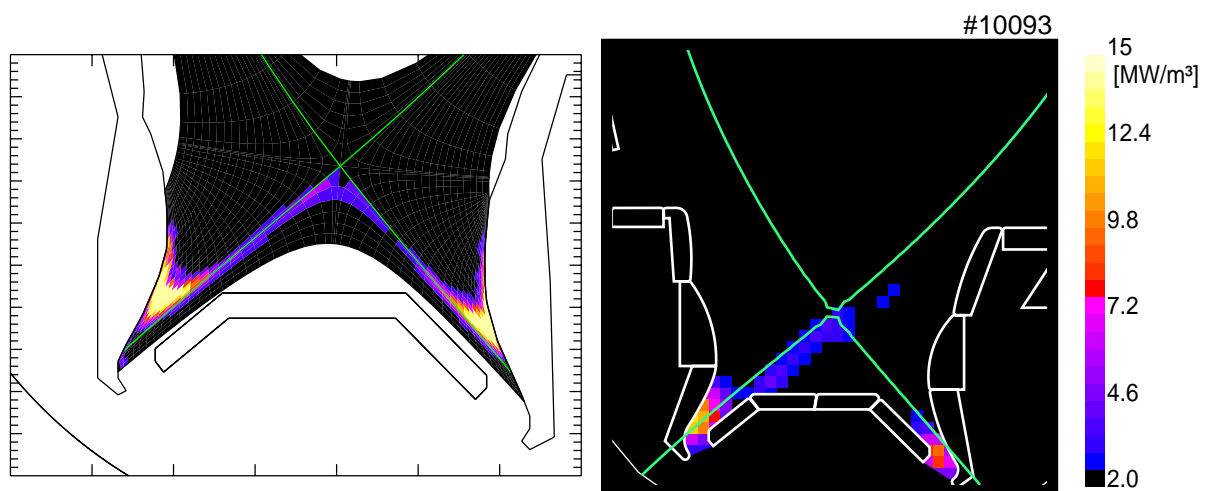


Fig. 4: a) B2-Eirene modeling of radiation distribution and b) reconstructed radiation distribution using virtual lines of sight show narrow radiation zone from strikepoints to X-point

that the region of interest was moved over several channels of the bolometer cameras. From the time evolution of the measured line integrals during the plasma shift several ‘virtual lines of sight’

were constructed and used for the reconstruction of the radiation pattern. Fig. 4b shows the result for a discharge with 5MW neutral beam injection power ($I_p=1\text{MA}$, $\bar{n}_e = 5.4 \cdot 10^{19}\text{m}^{-3}$, $B_T=2.5\text{T}$). The predicted radiation band is clearly seen with a width of a few centimeter and an emissivity of ca $3\text{-}4\text{MW/m}^3$ at the inner divertor. (Since there are no suitable lines of sight at the outer divertor yet, the corresponding band there cannot be detected.) Measurements from various spectrometers as well as modeling with B2-Eirene show that the radiation directly above the strike points originates from hydrogen and carbon (CII), and the radiation band consists mainly of carbon radiation, where CII, CIII, and CIV follow from the strikepoint to the X-point. [4,5]

Fig. 5 shows a comparison of the radiation distribution in the old DV-I and the new DV-II of ASDEX Upgrade for two similar L-mode discharges ($P_{NI} = 2.5\text{MW}$, $I_p=0.8\text{MA}$, $\bar{n}_e = 5 \cdot 10^{19}\text{m}^{-3}$). In DV-II there is more radiation than in DV-I, and it is more concentrated in the divertor fans. Also the radiation distribution in the divertor fans of DV-II is more symmetric than over the target plates of DV-I.

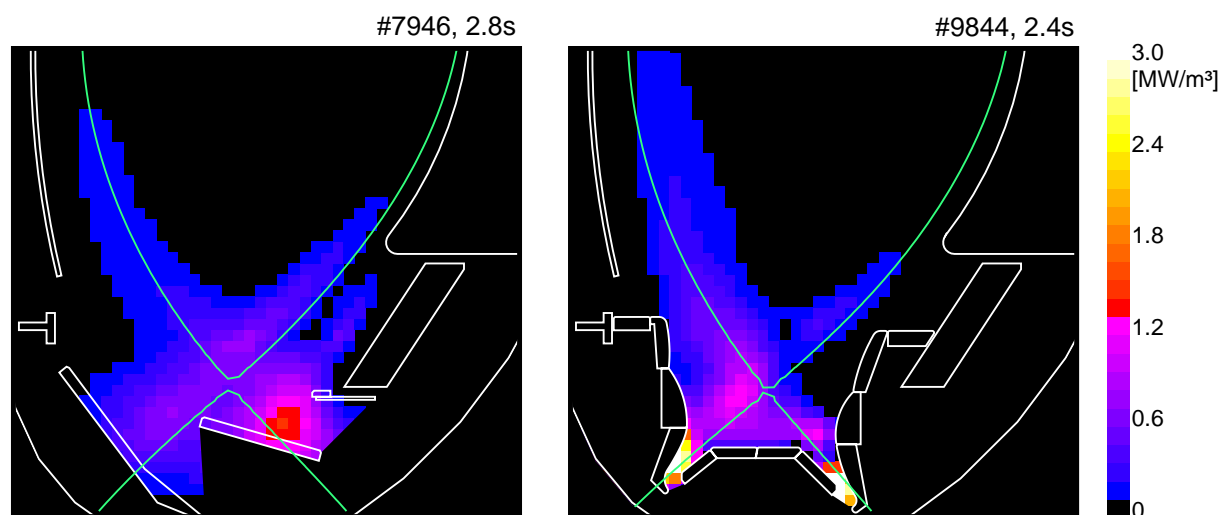


Fig. 5: Comparison of radiation distribution for DV-I (left) and DV-II (right)

3. Power Balance

Summing up input power, total radiated power measured by bolometers, power load on the divertor plates measured by IR-cameras, and the change of the MHD energy of the plasma, one arrives typically for all types of discharges (ohmic, L-, and H-mode) at a larger value than the input power (Fig. 2). However, parts of the divertor radiation are measured by both bolometer and IR-cameras. From the reconstructed radiation profile, one can calculate the radiated power onto the divertor plates. Correcting the power balance by this value, one arrives at a reasonably good power balance within 20% error bars.

Comparing the power density on the divertor plates measured by thermography with the radiation density on the plates calculated from the reconstructed radiation profiles, one finds that in the inner divertor a large part of the power load originates from radiation. In the outer divertor, however, radiation is only a small part of the power load on the divertor plates (Fig. 6).

4. Correction of the neutral gas pressure effects

Radiation losses from the inner and outer divertor leg in ASDEX Upgrade are measured with two pinhole cameras which are mounted under the roof baffle of the divertor, where high neutral

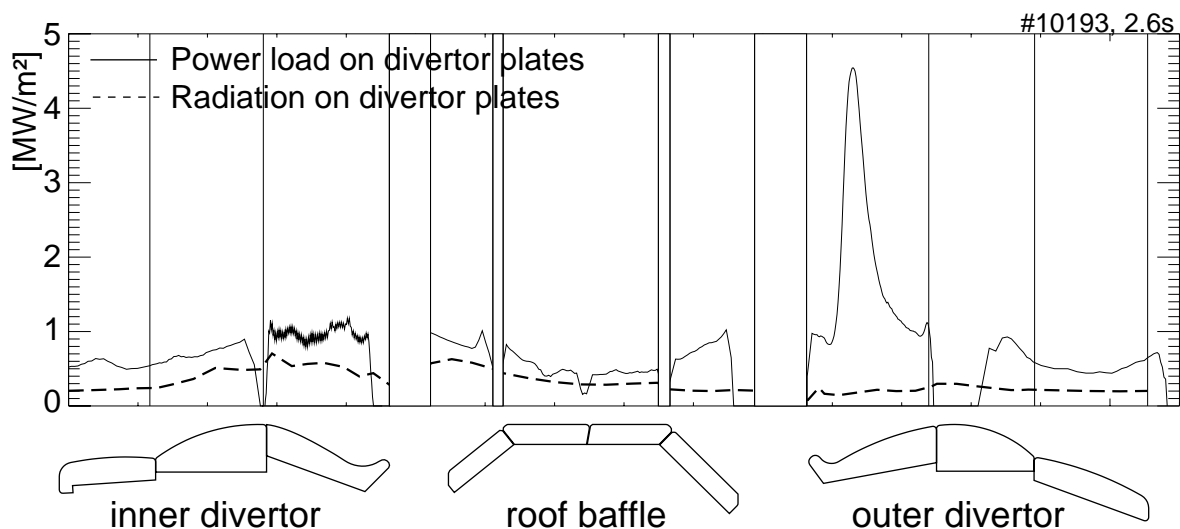


Fig. 6: Power load on divertor plates measured by thermography and radiation on plates calculated from the reconstructed profile for the 20MW discharge from Fig. 1

gas pressures of up to $5 \cdot 10^{-2}$ mbar arise during high power plasma discharges. Either of the two ‘roof baffle’ bolometer cameras is equipped with two various new bolometer heads recently developed in IPP which allow for a compensation of neutral gas pressure induced signal distortions of the bolometers. One is a four channel high impedance MICA bolometer head (NGC-bolometer) which effectively compensates the neutral gas pressure induced drift of the bolometer output signal. The other is a combined module which comprises three NGC-bolometers and one manometer based on the Pirani principle, which allows for a correction of the neutral gas pressure dependent bolometer sensitivity and of the residual bolometer offset drift.

A rather linear response of the manometer output voltage to the neutral gas pressure was found by an in-situ calibration with various gases in the ASDEX Upgrade vacuum vessel (Fig. 7). Simultaneously the residual offset drifts of the 14 roof baffle bolometers were measured as a function of the gas pressure which reveal linear dependencies, too. A simple correction of the offset drifts is routinely performed by subtracting the manometer output voltage multiplied with the individual constant calibration factors from the bolometer signals.

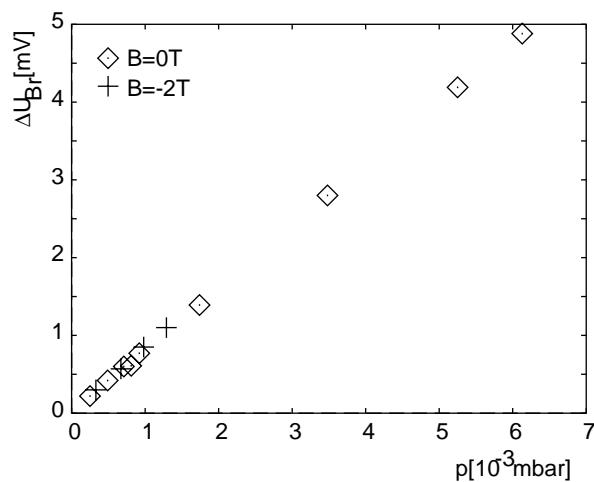


Fig. 7: Pressure dependence of the manometer output voltage for deuterium as working gas

References

- [1] K.F. Mast, J.C. Vallet, C. Andelfinger et al.: Rev. Sci. Instrum. **63**(3) (1991) 744
- [2] J.C. Fuchs, K.F. Mast, A. Herrmann, K. Lackner et al.: *Contrib. 21st EPS* (1994) 1308
- [3] A. Herrmann et al.: *this conference*
- [4] J. Gafert et al.: *this conference*
- [5] U. Wenzel et al.: *this conference*